NREL/TP-411-5326 • UC Category: 271 • DE93000071

NREL/TP--411-5326

DE93 000071

Growth Mechanisms and Characterization of Hydrogenated Amorphous-Silicon-Alloy Films

Annual Subcontract Report 14 February 1991 – 13 February 1992

A. Gallagher, R. Ostrom, G. Stutzin, D. Tanenbaum
National Institute of Standards and Technology
Washington, D.C.

NREL technical monitor: W. Luft

National Renewable Energy Laboratory
1617 Cole Boulevard
Golden, Colorado 80401-3393
A Division of Midwest Research Institute
Operated for the U.S. Department of Energy
under Contract No. DE-AC02-83CH10093

Prepared under Subcontract No. DD-H1001-1

February 1993

MASTER

DISTRIBUTION OF THIS DOCUMENT IS UNLIMITED

This publication was reproduced from the best available camera-ready copy submitted by the subcontractor and received no editorial review at NREL.

NOTICE

This report was prepared as an account of work sponsored by an agency of the United States government. Neither the United States government nor any agency thereof, nor any of their employees, makes any warranty, express or implied, or assumes any legal liability or responsibility for the accuracy, completeness, or usefulness of any information, apparatus, product, or process disclosed, or represents that its use would not infringe privately owned rights. Reference herein to any specific commercial product, process, or service by trade name, trademark, manufacturer, or otherwise does not necessarily constitute or imply its endorsement, recommendation, or favoring by the United States government or any agency thereof. The views and opinions of authors expressed herein do not necessarily state or reflect those of the United States government or any agency thereof.

Printed in the United States of America
Available from:
National Technical Information Service
U.S. Department of Commerce
5285 Port Royal Road
Springfield, VA 22161

Price: Microfiche A01
Printed Copy A03

Codes are used for pricing all publications. The code is determined by the number of pages in the publication. Information pertaining to the pricing codes can be found in the current issue of the following publications which are generally available in most libraries: *Energy Research Abstracts (ERA)*; *Government Reports Announcements* and Index (*GRA* and I); *Scientific and Technical Abstract Reports (STAR)*; and publication NTIS-PR-360 available from NTIS at the above address.

DISCLAIMER

Portions of this document may be illegible electronic image products. Images are produced from the best available original document.

SUMMARY

Goal:

The overall objective of this work is to better understand the atomic-scale structure of glow-discharge-produced a-Si:H, a-Ge:H, and a-Si:Ge:H films, its effect on film quality, and its dependence on deposition discharge conditions. A secondary objective is to establish a definitive, in-situ diagnostic of film quality that could be used to efficiently optimize process parameters in photovoltaic production systems. The approach taken is to measure the morphology and chemical characteristics of the as-grown film surface with atomic-scale resolution using a scanning tunneling microscope (STM). Many of the limitations of a-Si:H-based photovoltaics are attributed to microvoids, boundary defects, and microparticulate incorporation, and all of these should be visible at the surface of the growing film using STM.

Results:

During this year we completed construction of the discharge-deposition and surface-analysis apparatus, produced films, and diagnosed these with the scanning tunneling microscope (STM). We also achieved reliable operation of two methods of achieving atomically flat and clean substrates on which the films are deposited. We obtained STM scans of the topology of intrinsic a-Si:H surfaces, an achievement that required successful tunneling through this highly resistive material without destroying it. We initiated development of methods to produce the exceptionally sharp probe tips necessary for detecting small (nm-size) voids and protrusions on the growing surface of a-Si:H films. We have shown that a-Si:H grows uniformly, without islanding, on atomically clean crystal Si and GaAs, and we have studied the morphology of several thicknesses of these films. Due to the preliminary nature of these film surface observations, and the many different surface features and shapes seen, we have not yet drawn any conclusions regarding the causes of film quality variations or dependences on discharge conditions.

TABLE OF CONTENTS

Introduction	1
Technical Approach	1
Scanning Tunneling Microscopy	3
Tunneling Conditions	6
Background Tests	6
Probe Effects	7
Morphology of a-Si:H Film Surfaces	9
References	14

Figures

Fig. 1	Overall Apparatus Diagram	2
Fig. 2	STM Details	4
Fig. 3	Film Deposition Chamber	5
Fig. 4	Probe Convolution Examples	8
Fig. 5 & 6	STM Images of 100-Å-Thick a-Si:H Film Surfaces (T_s = 20°C)	11
Fig. 7 & 8	STM Images of 100-Å-Thick a-Si:H Film Surfaces (T_s = 20°C and 250°C)	12
Fig. 9	STM Images of 100-Å-Thick a-Si:H Film Surfaces (T_s = 250°C)	13

Introduction

The gas-phase plasma chemistry leading to glow-discharge a-Si:H film deposition has been studied rather thoroughly, and the primary mechanisms and species responsible for film growth are now fairly well understood.[1-4] Similarly, the electrical and related properties of this semiconducting film have been extensively diagnosed, and many characteristics are now fairly well understood.[5-7] In contrast there have been very few studies, and only vague models, of the growing film surface where the structural and electrical properties of the film are produced. Ellipsometry measurements[8,9] have investigated early-growth irregularities, and we have shown that the growing film has a very thin (1-2 atomic layers) hydrogen-rich surface.[10] However, such measurements detect surface averages, whereas structural irregularities are believed to be responsible for many key properties and limitations of a-Si:H photovoltaics.[11] Consequently, we have initiated this program, which is designed to measure the atomic morphology, and perhaps the individual species, at the growing film surface using a scanning tunneling microscope (STM). Kazmerski[12] and Wiesendanger et al.[13] have already obtained STM measurements of a-Si:H film surfaces, showing that atomic-scale species and morphology information can indeed be achieved on the surface of these amorphous materials. Our program is designed to carry this capability toward much more extensive measurements of many surface regions -- to alloys and to surfaces deposited under a variety of deposition parameters. It is commonly believed, from bulk-film measurements, that the critical electrical properties of these films are largely determined by their inhomogeneities, including those that occur rather infrequently.[11,14-16] Thus, extensive studies of many surface regions and deposition conditions appear necessary to elucidate the causes of the film structural features that limit photovoltaic efficiency and stability.

Technical Approach

We expect the initial atomic-scale morphology of C, Si, Ge, and H deposition from a glow discharge into a-Si:H and alloy films to depend strongly on the atomic-scale roughness and chemical composition of the substrate. To minimize the effect of such uncontrolled roughness and to optimize the connection to a large body of surface-science knowledge, we are initially studying a-Si:H and alloy-film deposition onto oriented, atomically smooth, and clean surfaces of crystal Si and GaAs. We also need to exclude the possibility of post-deposition contamination of the film surfaces. These constraints require ultra-high-vacuum (UHV) operation of the STM and other surface diagnostic equipment, and exacting sample preparation.

As shown in Fig. 1, the film deposition is done in an attached, turbomolecular pumped chamber, and film-coated substrates are transferred through a gate valve into the UHV chamber after termination of the glow discharge and deposition-gas flows. This pump down, sample cooling, and sample transfer into the STM typically requires ~30 minutes, during which time the sample is exposed briefly to $\sim 10^{-8}$ Torr and, thereafter, to $< 10^{-10}$ Torr of impurities (primarily H_2, CO, and CO_2) in the two chambers. This represents ~8 molecules per surface atom impinging on the surface before observation, which is not expected to

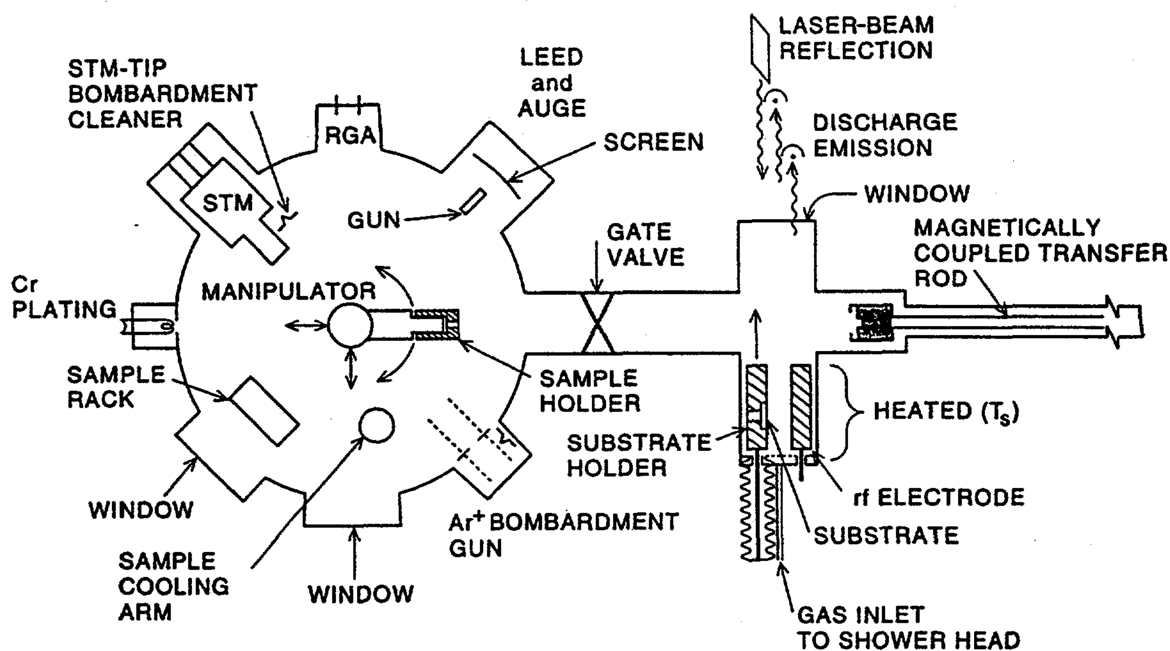

Fig. 1 Schematic of the film-deposition and diagnosis apparatus. The UHV chamber, left, is ion and Ti-sublimation pumped while the film-deposition chamber, right, is turbomolecular pumped. The substrate holder is moved after deposition as indicated by the arrow, so that the transfer rod can remove and transfer the substrate to the UHV manipulator.

significantly alter the exceptionally inert a-Si:H surface. (This is $\sim 10^{-13}$ of one day's exposure to the reactants in air.) Repeated and varied depositions on a single sample can be studied in this experimental arrangement without exposure to air. However, we do not yet have the ability to refind a particular location or feature after the film has been transferred back and forth between the deposition and UHV chambers. In essence, the STM only scans a region $\sim 0.5\ \mu m \times 0.5\ \mu m$, and our sample positioning is not sufficiently accurate to refind such a small area. Thus, following each deposition we randomly sample many areas on the surface.

Our film-deposition region is designed and operated to mimic conditions and arrangements most commonly used to produce device-quality a-Si:H and alloy films by glow-discharge deposition. However, the special requirement of sample transfer into the STM necessitates some unusual arrangements, as seen in a detail of the deposition region shown in Fig. 2. As shown there, the sample is mounted on a holder that is transferred between the discharge region and the STM. This holder also contains separate connections to two sides of the crystal to allow resistive heating during sample preparation. When film is deposited, the entire discharge region, shower head, and sample are heated to the substrate temperature. The rf electrode is 5-cm square and 2 cm from the substrate electrode, defining the discharge volume and yielding a relatively uniform discharge region at the sample. Deposition rate is measured with laser interference fringes and is normally ~ 3 Å/s.

Scanning Tunneling Microscopy

The core of the STM used here is shown diagrammatically in Fig. 3. This was originally made by McAllister Technical Services, based on a design by Lyding,[17] but it has been completely reconstructed and modified here, as the original instrument did not achieve atomic imaging in vacuum. The instrument now has two intravacuum stages of vibration isolation, a current amplifier at the probe tip, probe and sample cleaning attachments, coarse motion that allows observation of all regions of a sample, and a variety of other modifications. The substrate mount of Fig. 2 unscrews from the substrate electrode and screws into the cylindrical sample holder in Fig. 3. This cylinder is then slid into tunneling range along two horizontal rods, by a sawtooth motion of the outer piezoelectric tube. Once within tunneling range, the probe tip is moved in x, y, and z directions by the inner, quadranted tube piezo. The tungsten probe is removable, and is cleaned outside the STM but in the UHV by electron-bombardment heating. Atomically flat crystal Si samples are usually prepared by Shiraki cleaning, leaving a protective oxide layer that is thermally removed (~ 850 K) in vacuum. Atomically flat crystal GaAs is prepared by cleaving in vacuum; this produces some regions with many large and overlapping steps and other large atomically flat regions. We generally use tungsten wire probes, sharpened by electrochemical etching. There is a substantial literature and lore regarding probe-tip preparation methods and tip-end sharpness; we generally achieve probe-tip ends with ~ 200-Å radius and very rough, irregular shapes. We recently succeeded in producing much sharper probe-tip ends in situ, but none of the data presented here were obtained with such tips.

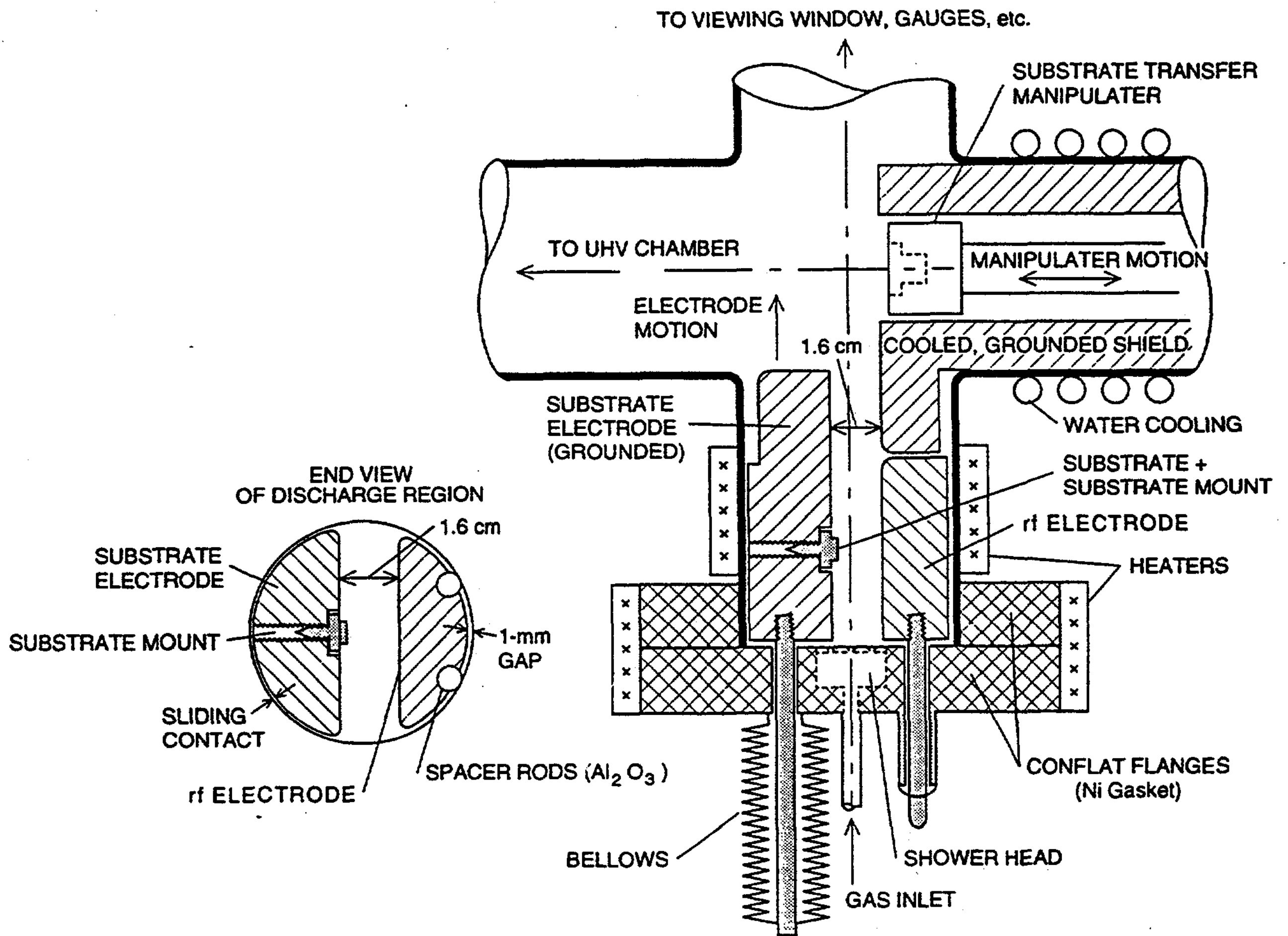

Fig. 2 Details of the glow-discharge film-deposition region. All materials are stainless steel, except as noted, plus the alumina rf-feedthrough insulator and a molybdenum substrate holder.

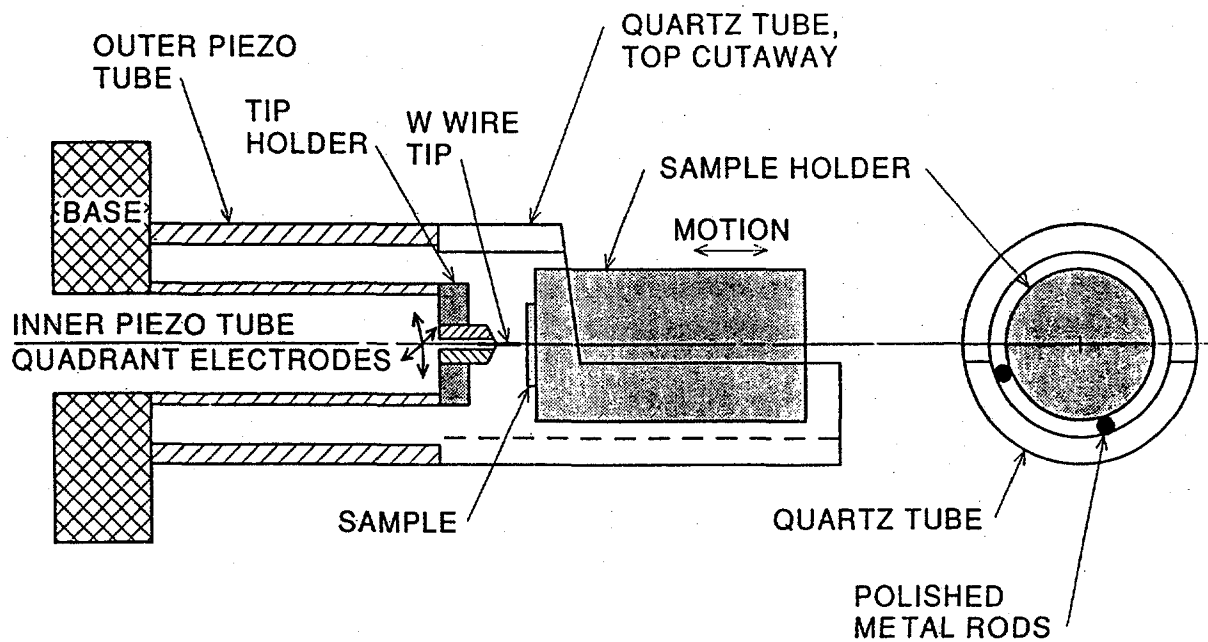

Fig. 3 Cross section and end view of the Lyding two-tube STM design, as adapted by McAllister in the STM we are using. The piezo tubes are 1.27-cm and 1.9-cm (0.5-in and 0.75-in) diameter.

Tunneling Conditions

An STM is normally operated with 10-pA to 1-nA tunneling current, passing through a 3-Å to 8-Å vacuum gap between the end of the probe and the sample. For high resolution measurements, with atomic-scale resolution, this current passes through a region on the order of 5-Å diameter. This enormous electron current density is easily sustained, without significant surface damage or voltage drop, by metal samples. However, in the case of crystalline semiconductors, it generally requires >2 V applied between the sample and metal probe to overcome the band bending and spreading resistance in the semiconductor. In the case of a-Si:H films, which are much less conductive than crystal semiconductors even when doped, it is not apparent how much voltage drop will occur in the film during tunneling. Consequently, we have had to study the dependence of tunneling and apparent surface topography on applied voltage and feedback current. Too low a voltage or too high a current results in surface damage by direct contact of the probe and sample, whereas too high a voltage induces sample and probe surface changes by atomic migration. We typically find that ~5 V and 10 pA is the best compromise for a 4000-Å thick film (~3 V for a 100-Å-thick film), where 10 pA is the lowest current that gives adequate bandwidth and signal/noise for our STM. We believe that a fraction of this voltage typically appears across the tunneling gap, and the remainder induces the necessary current density in the a-Si:H. The low-field conductivity of a-Si:H is insufficient to sustain the current density required for STM imaging, and a very large electric field induces the necessary current flow in the film. We have also investigated light biasing of the film conductivity, but this generally has a rather small effect because of the large field already present in the sample.

Background Tests

Because of the large height scale of film surface topology, compared to an atomic size, we always scan the surface in the constant-current tunneling mode. However, we frequently intersperse this with current (i) versus probe-height (z) data at a point. If the probe end penetrates the sample, as occurs with insufficient voltage or excessive current, this produces a very gradual and often irregular decrease in i(z). If excessive voltage is applied, this induces irregular z fluctuations versus time at a point, for constant current, due to atomic and bonding rearrangements. If the tungsten probe end is "dirty," or covered with nonmetallic atomic layers such as oxide or Si, then i(z) again falls relatively gradually as z is increased. When the probe tip is clean and current and voltage conditions are optimized, we observe stable z(t) at constant i and $i(z) \propto \exp(z/z_o)$, where the scale height z_o is <2 Å. This rapid current variation with z indicates the desired tunneling through a small vacuum gap between sample and probe; it also indicates that the topology obtained from a constant-current scan closely represents the actual surface shape. Different surface states at different sample positions can still produce apparent height variations, but these are expected to be small (<2 Å) under these circumstances. All data presented below were obtained under conditions that produced z_o <2 Å and "quiet" i(t).

Probe Effects

Probably the most difficult problem of scanning tunneling microscopy is the lack of control and knowledge of the atomic character of the probe end. Since tunneling through essentially a single atom on the probe end is necessary for high resolution, the properties of the surface atomic layers are crucial to the tunneling behavior. The vacuum barrier height (ϕ) is a sensitive function of surface structure, surface states, and surface contamination. Combined with the gap dependence on ϕ, any fluctuation in surface atomic positions or couplings, or in species, causes gap fluctuations. Such z fluctuations or "noise" are invariably seen, but with varying size and frequency at different times. Similarly, transverse resolution varies when the atomic arrangement of the tip changes. These variations in noise and resolution are usually attributed to atomic changes in the probe tip, and it is common practice to ignore all but periods of relatively high resolution and quiet data when a "good" probe tip occurs. There are many prescriptions for cleaning and otherwise obtaining "good" tips. These include deliberately pressing or scraping the tip into the sample, applying a voltage pulse to move or transfer atoms, waiting for a gas impurity to adhere to the tip, heating the probe, and scanning the sample until a "good" tip miraculously appears. (Of course, one can move to a new sample area after exercising any procedure that damages the sample surface.) We have used all of these at various times, but some sample surfaces are not very robust, and it is quite easy to damage the a-Si:H surface and to transfer material from a-Si:H films to the probe. The i(z) data described above, combined with i(V) and resolution measurements, are used to determine when a stable and "good" tip condition is obtained. The topology data presented were obtained from such tips. (Transverse resolution is apparent in the scan data.)

A second probe effect results from the fact that the data represent a convolution of probe surface with the sample surface, at a fixed spacing of typically ~5 Å. This is not particularly important in studies of essentially atomically flat crystal surfaces, as the surface height varies by only a few angstroms. However, it is crucial when looking for nanometer-size irregularities and incipient voids on the surface of a-Si:H films. An example of this convolution effect is shown in Fig. 4a, for a probe-tip shape representative of the best obtainable from normal electrochemical etching of tungsten. Note that sample protrusions appear broadened, but with true height, while sample valleys appear with decreased height and width. In order to see incipient sample voids of <200-Å width without excessive distortion, a probe-tip shape similar to that in Fig. 4b is needed. Our need for a narrow, sharp probe end is relatively unusual, and no straightforward or well-tested methods exist for producing or diagnosing such probe ends. For this reason, we recently devoted a major effort to developing methods to measure the shape of the probe end and produce very sharp ends. This was successful, and we are able to place tall, narrow columns with ~10-Å end radius on the end of a probe, similar to that seen in Fig. 4b. However, this is not yet a simple or a rapid procedure, and it requires changing to a crystal-Si sample and making certain that no atomic changes to the tip result from subsequently approaching and scanning the a-Si:H films. Consequently, we have not yet used these sharper probe tips with a-Si:H films.

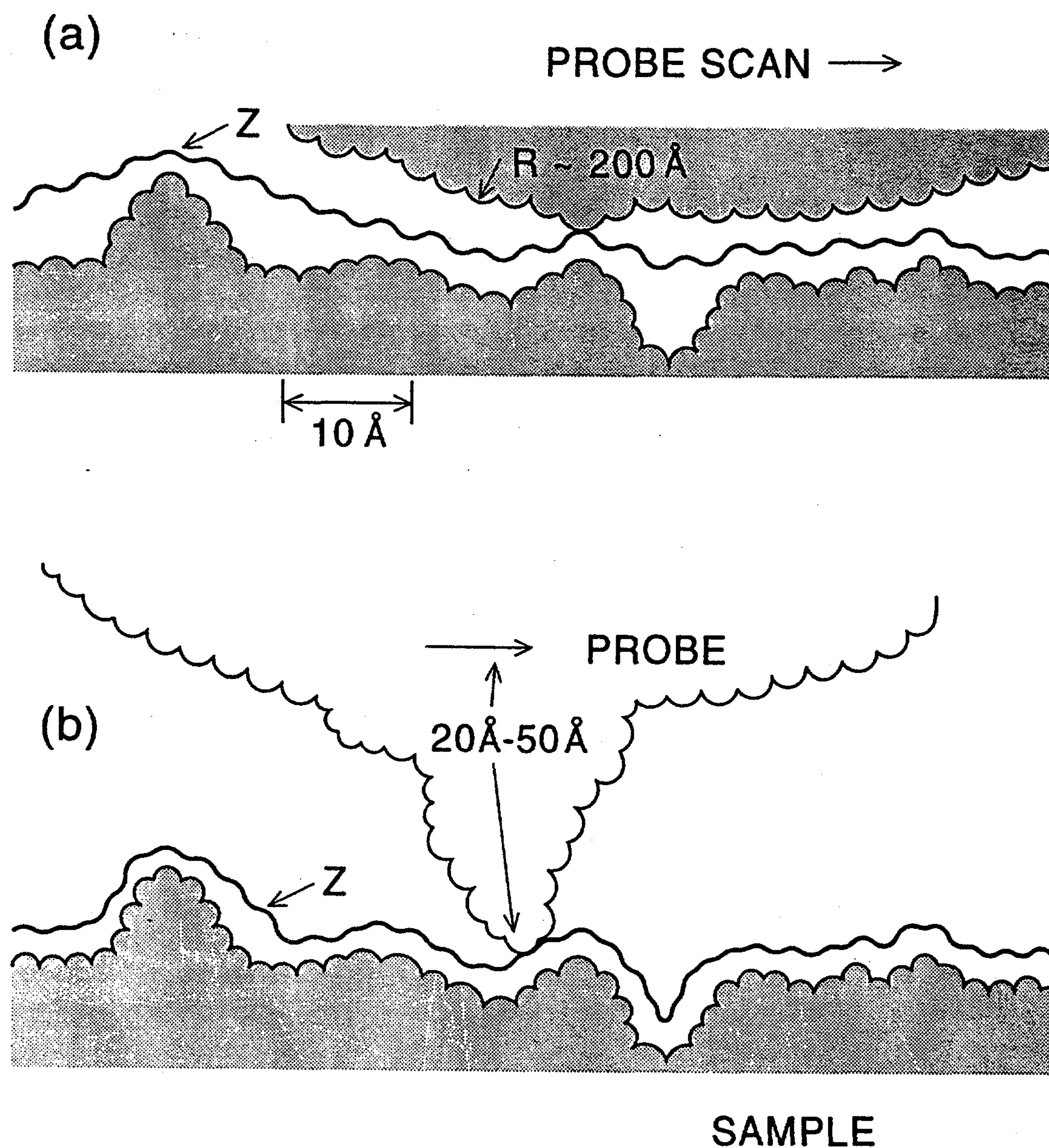

Fig. 4 Two examples of the probe-sample convolution that occurs in scanning tunneling microscopy. The heavy line labeled Z is the recorded scan line that results from scanning the probe (above) across the sample (below) at a fixed separation. (a) A typical probe end obtained by electrochemical etching of tungsten. (b) A probe tip of the form prepared in our laboratory by adding material to the probe tip, using carefully controlled voltage pulsing above a crystal-Si surface.

When we use normally etched probe tips, as in the data presented here, the spatial resolution of the probe must be inferred as accurately as possible from the observed topology of the surface. The width (W) of the sharpest upward protrusion detected anywhere on any scan of the surface yields an upper limit for the shape of the probe end (e.g., Fig. 4a). Observed valleys will then be narrower than their true width by some fraction of W (see Fig. 4b). In essence, every data set must be analyzed with care to avoid misleading interpretations.

Morphology of a-Si:H Film Surfaces

We have so far studied intrinsic a-Si:H film growth on crystal Si and GaAs, concentrating on atomic-scale irregularities and the smoothness of the initial film growth. The film is deposited at T_s = 25° or 230°C on the grounded electrode of a rf silane discharge. The silane flow is 10-15 sccm, and the entire tube and both electrodes are heated. The silane pressure, at 240°C, is typically 0.4 Torr, and the film deposition rate on the substrate is 1-3 Å/s. These conditions of deposition rate or power density, power/flow, T_s = 240°C, and pressure multiplied by gap closely correspond to those used at most facilities to produce the highest (device) quality intrinsic a-Si:H layers for photovoltaics by rf glow discharge. No discharge-produced Si particulates are visible on electrode or downstream surfaces for these conditions, but they do appear at the throttle valve when the power/flow is increased by a factor of ~5.

The atomic-scale morphology of the surface of a 100-Å layer of a-Si:H film on an atomically flat Si (111) crystal is shown in Figs. 5-7 for T_s = 25°C. Figures 5-7 are typical of many different regions of the surface that were scanned with similar resolution. In essence, most 100-Å square regions of the surface are flat within one atomic layer (3 Å), but occasional protrusions or troughs several angstroms in height are seen, as in Fig. 7. The larger-scale topology contains gradual undulations, as seen in Fig. 5. There is no indication of incipient voids, as might have been expected on the basis of reports of voids measured in bulk films. For the limited number of ~3,000-Å square surface regions that have been studied so far, no micro or nano particulates (dust) have been observed on this as-grown surface. Occasionally, a large-scale irregularity in the surface flatness has been detected, but this is attributed to a flaw in the crystal Si surface polish that is not smoothed out by the thin-film layer. Surface flaws are very dense on most substrates, and this implies that these may propagate considerable distances into the film before being smoothed out.

Figures 8 and 9 show the typical surface topology of a 100-Å layer of a-Si:H grown at 2.4 Å/s on a GaAs crystal at T_s = 250°C. The vacuum-cleaved crystal surface is atomically flat and clean, while the a-Si:H surface typically has ~10-Å total height variations, as seen in the figures. At the top of Fig. 5, a single scan line is shown with a highly expanded vertical scale. This scan line passes through the sharpest depression in this particular image, seen as a dark spot. This depression, marked by an arrow, is 6-Å deep and ~35-Å wide at the top; the sides slope ~20° to the horizontal. Thus, even this depression is a very open trough, far from that which might be expected to initiate a void with further film growth. This region is representative of many scanned regions of the film surface.

As described above, these STM images are a convolution of the shapes of the probe end and of the substrate surface, typically at ~5-Å gap. The probe end normally has a radius of 100 Å - 300 Å, so a relatively steep-sided surface trough or protrusion, compared to the probe end, may not be observable in the image. In the present studies of a-Si:H surface morphology, we are looking for just such small troughs and protrusions, so it is imperative to use a probe with a very sharp end.

For the images in Figs. 5-9, we relied on a variety of other STM images obtained with the same probe to indicate the detectability of small features. Based on the sharpest features seen in any image using a particular probe, we found that the probe-end shape used for the above data could produce features of up to 10-Å height or depth with ~45° surface slope. This was sharper than almost all features seen on the a-Si:H surfaces at that time, as can be seen in the examples in Figs. 5-9. Thus, it appears unlikely that we missed any narrow surface troughs or protrusions due to the relatively blunt probe end. However, these were only ~100-Å thick layers of a-Si:H, and larger voids might be more common in thicker films. We now hope to be able to discern these using probes with tall, sharp structures on the end.

These preliminary studies show that intrinsic a-Si:H film grows very homogeneously and smoothly on a flat substrate under typical "optimum" deposition conditions. No indications of particulate deposition or of >10-Å diameter nanoparticles have yet been seen.

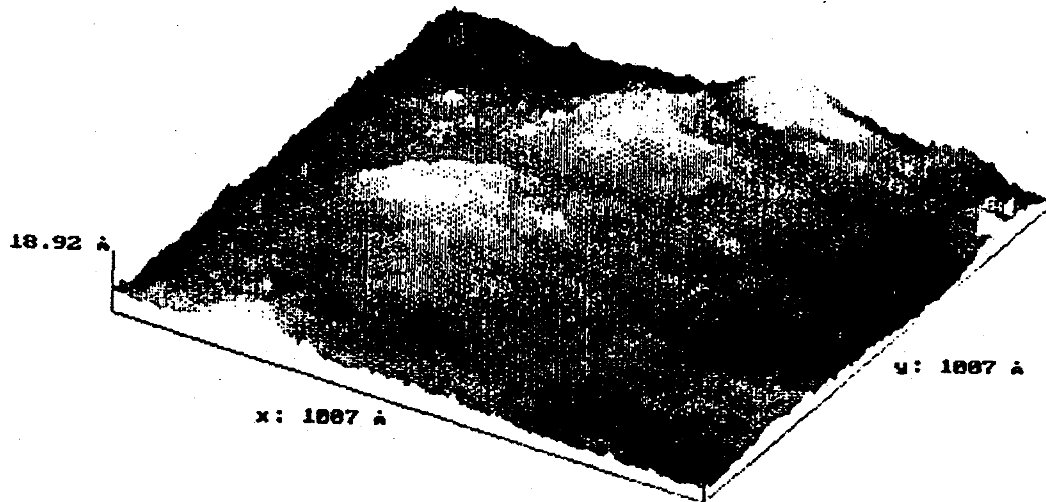

Fig. 5 STM image of a 100-Å thick, T_s=20°C, a-Si:H film deposited on a Si(111) crystal surface

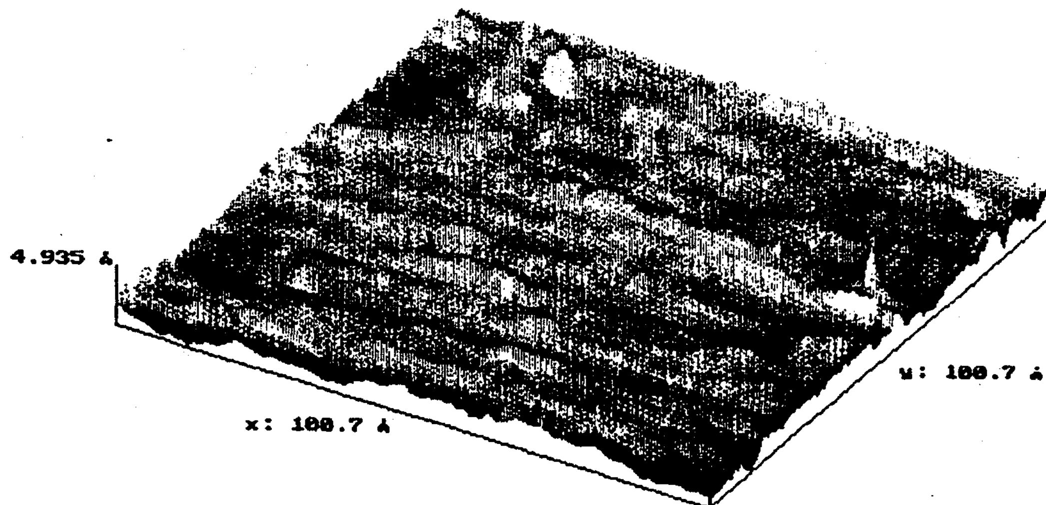

Fig. 6 STM image of a different region of the a-Si:H film in Fig. 5

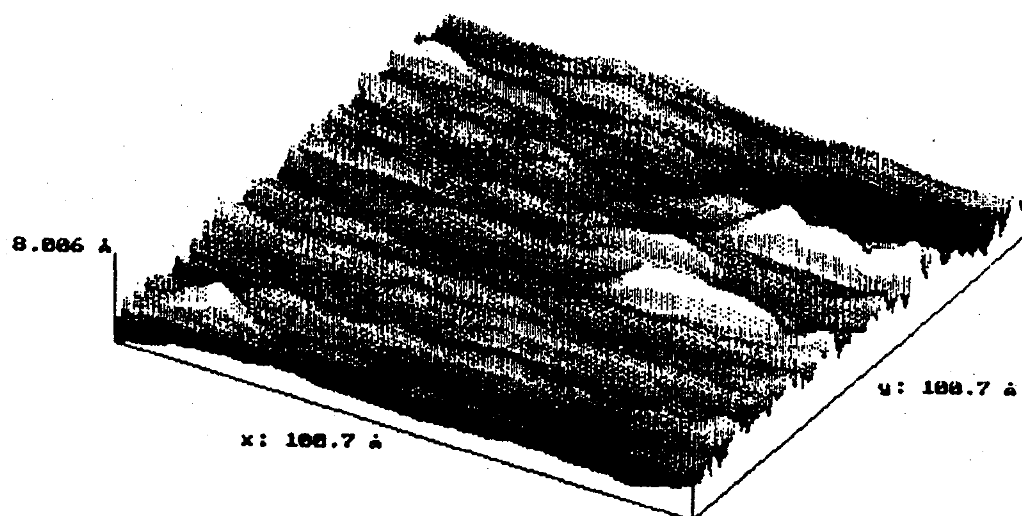

Fig. 7 STM image of another region of the a-Si:H film shown in Fig. 5

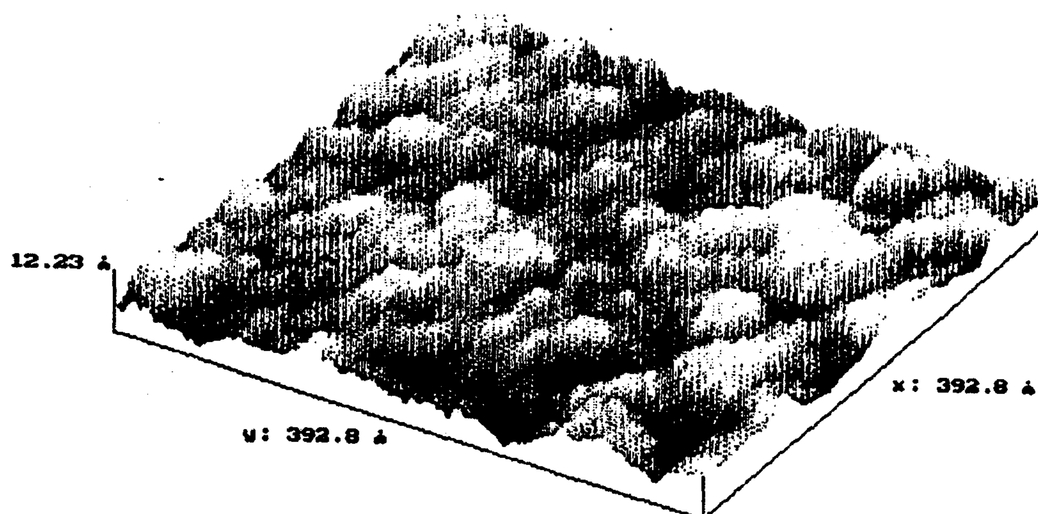

Fig. 8 STM image of the surface of a 100-Å thick a-Si:H film grown on atomically flat, crystal GaAs at T_s=250°C

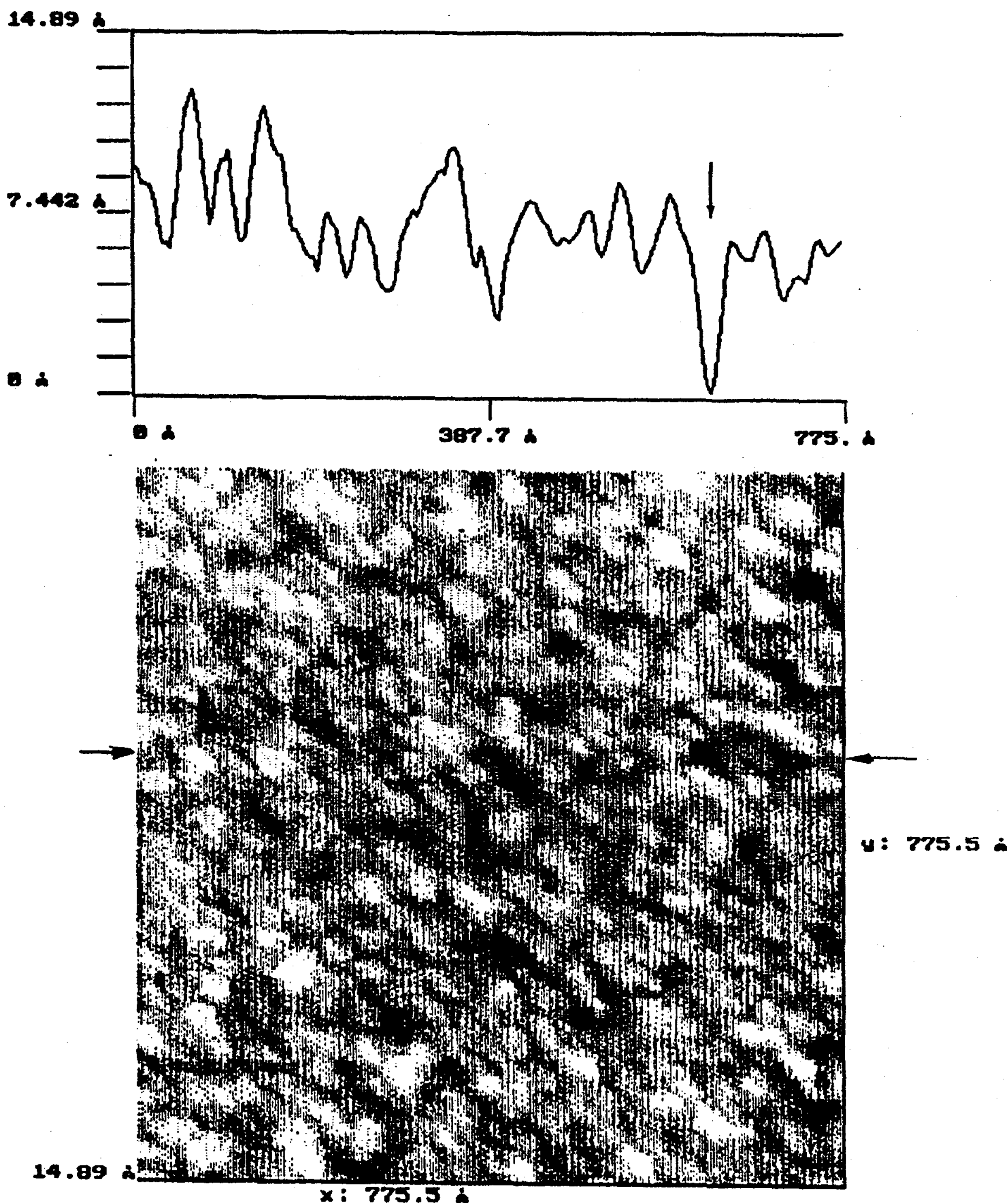

Fig. 9 STM image of a 100-Å thick a-Si:H film grown on crystal GaAs at T_s=250°C. The dark-to-white-shading scale represents a 14-Å height range. A single scan line across the image, at the location indicated, is shown at the top of the figure.

References

1. D. A. Doughty and A. Gallagher, J. Appl. Phys. 67, 139 (1990).
2. J. R. Doyle, D. A. Doughty, and A. Gallagher, J. Appl. Phys. 68, 4375 (1990).
3. N. Itabashi, N. Nishiwaki, M. Magane, S. Naito, T. Goto, A. Matsuda, C. Yamada, and E. Hirota, Jpn. J. Appl. Phys. 29, L505 (1990).
4. T. Goto, Ed., *Proceedings of the International Seminar of Reactive Plasmas* (Organizing Committee of the International Seminar on Reactive Plasmas, Nagoya, Japan, 1991).
5. J. D. Joannopoulos and G. Lucovsky, Eds., *The Physics of Hydrogenated Amorphous Silicon, I and II, Topics in Applied Physics* (Springer, Berlin, 1984), Vols. 55, 56.
6. E. F. Demichelis, Ed., *Physics and Application of Amorphous Semiconductors* (World Scientific, Singapore, 1988).
7. B. L. Stafford, Ed., *Amorphous Silicon Materials and Solar Cells*, AIP Conf. Proc. 234 (AIP, New York, 1991).
8. R. W. Collins and J. M. Cavese, J. Appl. Phys. 61, 1869 (1987).
9. B. Drevillon and R. Benferhat, J. Appl. Phys. 63, 5088 (1988).
10. G. H. Lin, J. R. Doyle, M. He, and A. Gallagher, J. Appl. Phys. 64, 188 (1988).
11. A. H. Mahan, D. L. Williamson, B. P. Nelson, and R. S. Crandall, Phys. Rev. B 40, 12024 (1989); Solar Cells 27, 465 (1989); Appl. Phys. Lett. 55, 783 (1989).
12. L. L. Kazmerski, Ninth E. C. PV Solar Energy Conf., Freiburg, Germany, September 25, 1989.
13. R. Wiesendanger, L. Rosenthaler, H. R. Hidber, H. J. Güntherodt, A. W. McKinnon, and W. E. Spear, J. Appl. Phys. 63, 4515 (1988).
14. H. Wagner and W. Beyer, Solid State Commun. 48, 585 (1983).
15. P. C. Tayler, in *Semiconductors and Semimetals, Vol. 21C: Hydrogenated Amorphous Silicon*, J. I. Pankove, Ed. (Academic Press, Orlando, 1984), p. 99.
16. V. P. Bork, P. A. Fedders, D. J. Leopold, R. E. Norberg, J. B. Boye, and J. C. Knights, Phys. Rev. B 36 9351 (1987).
17. J. W. Lyding, S. Skala, J. S. Hubacek, R. Brockenbrough, and G. Gammie, Rev. Sci. Instrum. 59, 1897 (1990).

Document Control Page	1. NREL Report No. NREL/TP-411-5326	2. NTIS Accession No. DE93000071	3. Recipient's Accession No.

4. Title and Subtitle Growth Mechanisms and Characterization of Hydrogenated Amorphous-Silicon-Alloy Films	5. Publication Date February 1993
	6.
7. Author(s) A. Gallagher, R. Ostrom, G. Stutzin, D. Tanenbaum	8. Performing Organization Rept. No.
9. Performing Organization Name and Address National Institute of Standards and Technology	10. Project/Task/Work Unit No. PV241104
	11. Contract (C) or Grant (G) No. (C) DD-H1001-1 (G)
12. Sponsoring Organization Name and Address National Renewable Energy Laboratory 1617 Cole Blvd. Golden, CO 80401-3393	13. Type of Report & Period Covered Technical Report 14 February 1991–13 February 1992
	14.

15. Supplementary Notes
NREL technical monitor: W. Luft

16. Abstract (Limit: 200 words)

This report describes an apparatus, constructed and tested, that allows measurement of the surface morphology of as-grown hydrogenated amorphous silicon films with atomic resolution using a scanning tunneling microscope. Surface topologies of 100-Å-thick intrinsic films, deposited on atomically flat, crystalline Si and GaAs, are reported. These film surfaces are relatively flat on the atomic scale, indicating fairly homogeneous, compact initial film growth. The effect of probe-tip size on the observed topology and the development of atomically sharp probes is discussed.

17. Document Analysis
a. Descriptors
characterization ; amorphous silicon ; alloy ; films ; photovoltaics ; solar cells

b. Identifiers/Open-Ended Terms

c. UC Categories
271

18. Availability Statement National Technical Information Service U.S. Department of Commerce 5285 Port Royal Road Springfield, VA 22161	19. No. of Pages 19
	20. Price A03

Form No. 0069E (6-30-87)